Article ID: 1000-324X(2021)10-1111-07 **DOI:** 10.15541/jim20210045

Influence of SiC Nanowires on the Damage Evolution of SiC_f/SiC Composites

LI Longbin[1,2], XUE Yudong[1,2], HU Jianbao[1,2], YANG Jinshan[1,2], ZHANG Xiangyu[1,2], DONG Shaoming[1,2]

(1. State Key Laboratory of High Performance Ceramics and Superfine Microstructure, Shanghai Institute of Ceramics, Chinese Academy of Sciences, Shanghai 200050, China; 2. Center of Materials Science and Optoelectronics Engineering, University of Chinese Academy of Sciences, Beijing 100049, China)

Abstract: SiC fiber (SiC_f)/SiC composites were modified by SiC nanowires (SiC_{nw}) grown *in-situ* on SiC fiber to obtain hierarchical structure. Effects of this hierarchical structure on the properties of composites, such as microstructure, fracture strength and damage evolution, were evaluated. Results show that the introduction of SiC_{nw} significantly improves the matrix infiltration efficiency. SiC_{nw} and BN-coated SiC_{nw} reinforced SiC_f/SiC composites acquire better performance in bending tests by comparison with conventional SiC_f/SiC. SiC_{nw} coated by BN interphase obviously enhances the strength owing to weak-bonded interface. Besides, results of acoustic emission and Coated Vickers Hardness Impresses reveal that SiC_{nw} delay early damage evolution at early state and mainly make contribution to hindering and bridging of microcracks, which is further enhanced by BN-coated SiC_{nw}.

Key words: hierarchical composites; SiC nanowire; mechanical properties; acoustic emission

Among various types of continuous fibre reinforced ceramic matrix composites (CMCs), SiC fiber (SiC_f)-reinforced SiC matrix composites (SiC_f/SiC) with superior mechanical and thermal properties have obtained increasing attention in industrial applications like aerospace, nuclear and braking system over past few decades[1-3]. However, major issues like sensitivity to structural defects and brittle behavior in external load require effective solution for optimizing the performance of SiC_f/SiC in application[4]. Nanotubes-reinforced hierarchical composites introduce a practicable way to handle the issues due to their significant improvement in toughness and strength[5]. Nanotubes such as carbon nanotubes (CNTs) and boron nitride nanotubes (BNNTs) present better mechanical properties by enhancing brittle microstructural parts relatively away from fiber bundles, monolithic composites are efficiently toughened and strengthened owning to ductile behavior like sliding, pull-out and bridging of these micro-scale counterparts of fibers[6-7]. Apart from CNT and BNNT, SiC_{nw} and SiC whisker with high tensile modulus and strength also acquire good performance as hierarchical reinforcement in both C_f/SiC and SiC_f/SiC composites owing to their restriction effect on crack propagation in and into fiber bundles[8].

However, research on the mechanism of toughening and strengthening of SiC_{nw} is still not rich enough to elaborate the effect on mechanical behavior of hierarchical composites under external load. According to previous study[9], the mechanical improvements of SiC_{nw} reinforced C_f/SiC composites were mainly attributed to crack deflection and bridging of SiC nanowires as well as their pull-out and sliding effect in the matrix. In our work, acoustic emission (AE) was introduced to monitor the damage evolution in real time,Vickers Hardness Impresses was employed to evaluate the propagation of obvious transverse cracks. As the mechanical behavior and fracture mechanism of SiC_f/SiC composites modified with SiC_{nw} is still unclear, this study is expected to show a better understanding of SiC nanowire as a mechanical reinforcement.

1 Experimental

1.1 Preparation of materials

SiC_{nw} were *in situ* grown on SiC fiber (KD-II, with 500 nm thick BN interphase deposition in advance) surface after 10 h Ni^{2+} solution treatment by chemical vapor

Received date: 2021-01-27; **Revised date:** 2021-04-15; **Published online:** 2021-05-10
Foundation item: National Science and Technology Major Project (2017-IV-0005-0042); Key Research Program of Frontier Science, Chinese Academy of Sciences (QYZDY-SSW-JSC031)
Biography: LI Longbin(1997–), male, Master candidate. Email: medolia97@student.sic.ac.cn
李陇彬(1997–), 男, 硕士研究生. E-mail: medolia97@student.sic.ac.cn
Corresponding author: DONG Shaoming, professor. E-mail: smdong@mail.sic.ac.cn
董绍明, 研究员. E-mail: smdong@mail.sic.ac.cn

infiltration (CVI). H_2 (30 sccm) and methyl trichlorosilane (MTS, 100 sccm) were utilized as reductant as well as source gas. The growth of SiC_{nw} was carried out under a pressure of 2 kPa at 1000 ℃ for 1 h. To achieve the optimum of SiC_{nw}/matrix interfacial bonding, BN interphase was deposited on SiC_{nw} surface *via* chemical vapor deposition (CVD) method at 800 ℃ using BCl_3 (10 sccm) and NH_3 (20 sccm).The composites were densified using precursor impregnation and pyrolysis (PIP) method. Finally, original SiC_f/SiC composites, as-grown and BN-coated SiC_{nw} modified SiC_f/SiC hierarchical composites were fabricated. These composites were marked as SiC_f/SiC, SiC_f/SiC-SiC_{nw} and SiC_f/SiC-SiC_{nw}/BN, respectively.

1.2 Characterizations

The bulk density and open porosity were evaluated by the Archimedes principle. Three-point bending test was performed on a CRIMS-DDl20 universal testing machine with a span of 30 mm at a cross head speed of 0.1 mm/min. Composites were cut into bar specimens with the dimension of 2.0 mm×4.0 mm×40 mm for bending test. AE technique was employed to detect *in situ* information of damage process in composites during the three-point bending test. AE activity, containing the information of damage events, was real-timely recorded. AE detection was conducted by using a two-channel MISTRAS acquisition system (Physical Acoustics Corporation) with a sampling rate of 2 MHz. Two nano-30 (Physical Acoustics Corporation) sensors were mounted on the surface of specimens to record AE signals. Two pre-amplifiers were also adopted and set with the pre-amplification of 40 dB and band-pass filtering of 20–1200 kHz. To avoid possible noise recording, the threshold was set at 45 dB (as shown in Fig. 1). Hitachi SU8220 field-emission scanning electron microscope (SEM) were used to characterize the morphology and microstructure of as-grown and BN-coated BNNTs. The fracture morphology of fibers in composites were also investigated *via* SEM. The Vickers Hardness Impresses was applied to induce the crack formation of SiC_{nw}/SiC matrix by a Vickers hardness tester (HVS-5) with a load of 500 g for 10 s, and the crack propagation was observed by SEM.

2 Results and discussion

2.1 Microstructure

The morphologies of fibers covered by SiC_{nw} before matrix infiltration are shown in Fig. 2. As seen in Fig. 2(a-c), the microscale network composed of SiC_{nw} filled the gap between fiber bundles which surfaces are barely exposed. The length of nanowires as secondary reinforcement is approximately 10–20 μm and the diameter is about 60–100 nm. Macroscopic properties like density and porosity for each group are listed in Table 1. Compared to original SiC_f/SiC, the density of composite SiC_f/SiC-SiC_{nw} increases from 1.98 g/cm^3 to 2.08 g/cm^3, and the open porosity decreases from 17.64% to 11.58%. Combined

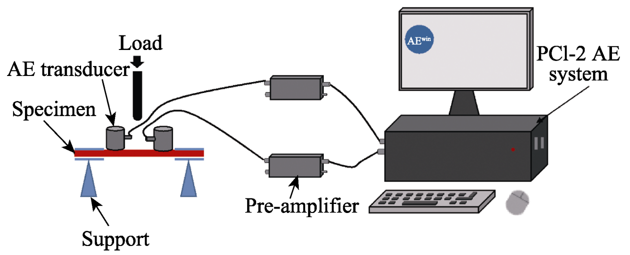

Fig. 1 Schematic figure of three-point test with *in-situ* AE monitoring system

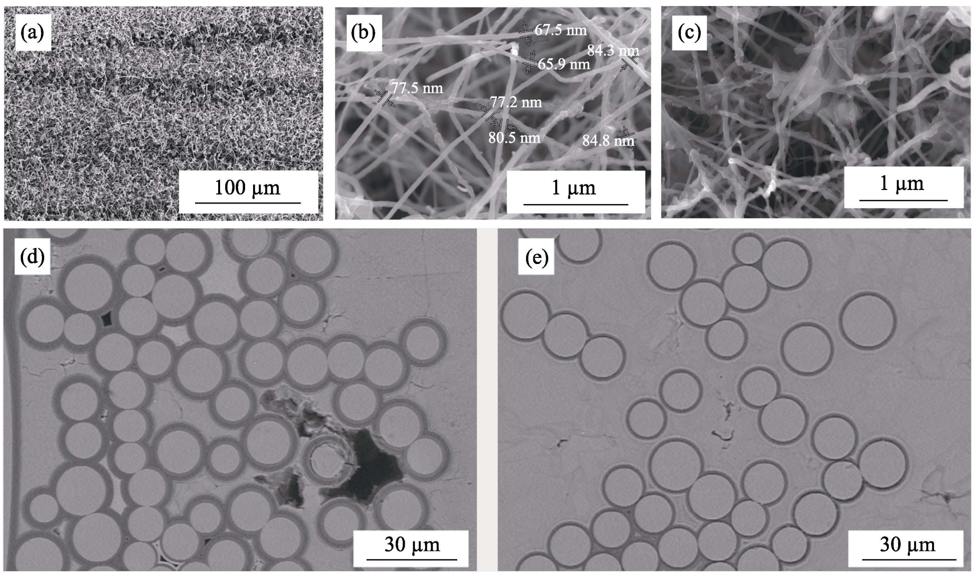

Fig. 2 Typical SEM images of (a, b) as-grown SiC_{nw}, (c) BN-coated SiC_{nw}, and typical SEM images demonstrating the pore size of (d) SiC_f/SiC and (e) SiC_f/SiC-SiC_{nw} composites

with Fig. 1(d, e) demonstrating the pores in fiber bundles, it indicates that the incorporation of SiC_{nw} densifies the monolithic composite by suppressing the formation of large-sized micro-pores. ZHAO *et al*.[10] studied similar structure and concluded that this network was preferred due to less possibilities to cause undesirable clogging in the matrix infiltration process and simultaneous enough strength for enhancing microdomains near or between fiber bundles.

The aim of deposition of BN interphase on SiC_{nw} is to render composites more optimized mechanical strength, since the direct contact between SiC nanowires and matrix leads to an undesirable strong bond[11]. Moreover, the influence of weak-bonded interface between nanowires and matrix on damage evolution requires investigation in detail.

2.2 Mechanical properties and fracture morphologies of composites

Mechanical properties of these composites are evaluated and gathered in Table 2. It can be implied that SiC_{nw} as secondary reinforcement indeed produce positive influence on mechanical behavior. Flexural strength of SiC_f/SiC-SiC_{nw} and SiC_f/SiC-SiC_{nw}/BN is 15.7% and 42.1% higher than that of original SiC_f/SiC, respectively, which may be attributed to the strengthening effect of nanowires in and between fiber bundles, as shown in Fig. 2. This impact is further intensified by deposition of BN interphase on the surface of nanowires. The fracture morphologies of each group are shown in Fig. 3 and Fig. 4. As discussed above, direct contact of nanowires with matrix causes a strong interfacial bond. It can be confirmed by the observation in Fig. 3(a) that few pull-outs of nanowires are found. Instead of tending to be pulled out, nanowires prefer to breaking. On the contrary, obviously much more pull-outs are inspected in composites SiC_f/SiC-SiC_{nw}/BN, as illustrated in Fig. 3(b). Furthermore, a local part of Fig. 3(b) is magnified in Fig. 3(c), indicating that nanowires are easier to be pulled out with assistance of weaker interfacial bonding. Fig. 4 demonstrates different fracture morphologies of fibers in three types of composites. It can be concluded that fiber/matrix interfacial bonding is exceedingly enhanced after introducing SiC_{nw}, for the SiC_f/SiC-SiC_{nw} shows apparent brittle fracture mode in Fig. 4(a). However, above mentioned effect is effectively alleviated by introducing BN interphase, phenomenon of long pull-outs of fibers happens again in SiC_f/SiC-SiC_{nw}/BN, indicating better mechanical performance for material after the formation of obvious transverse cracks[12].

It is noticeable that the strain at maximum load for composites SiC_f/SiC-SiC_{nw} is relatively bigger than that for original SiC_f/SiC, a possible explanation could be illustrated as following. In general, the failure strain of composites is mainly decided by fiber/matrix bond and stress status in fibers. The SiC_{nw}/matrix strong bond may help load transfer among fibers, and improve their ability to bear load. Therefore, load concentration of fibers is reduced and break of fibers is delayed, causing bigger failure strain in composites SiC_f/SiC-SiC_{nw}. However, stronger evidence requires more profound study.

As inspiration of this research, the restriction effect of nanowires on the formation and evolution of matrix cracks was observed and significantly benefits fracture

Table 1　Density and porosity of different composites

Composite	SiC_f/SiC	SiC_f/SiC-SiC_{nw}/BN	SiC_f/SiC-SiC_{nw}
Bulk density/(g·cm^{-3})	(1.98±0.03)	(2.02±0.04)	(2.08±0.03)
Open porosity/%	(17.64±1.08)	(14.39±0.60)	(11.58±1.35)

Table 2　Properties of original composites, as-grown and BN-coated hierarchical composites

Composite	SiC_{nw} content / wt%	Flexural strength, σ_u/MPa	Proportional limit stress, σ_{PL}/MPa	Strain at flexural strength, ε_u/%	First AE stress, σ_{min}/MPa	AE onset stress, σ_{onset}/MPa
SiC_f/SiC	0	(356.7±16.2)	(153.9±6.4)	(0.39±0.05)	(58.8±7.5)	(116.1±8.9)
SiC_f/SiC-SiC_{nw}	2.0	(412.6±22.4)	(185.1±7.7)	(0.63±0.06)	(66.1±6.2)	(155.8±7.7)
SiC_f/SiC-SiC_{nw}/BN	2.0	(506.4±28.3)	(247.7±8.6)	(0.88±0.12)	(78.5±5.2)	(171.6±15.9)

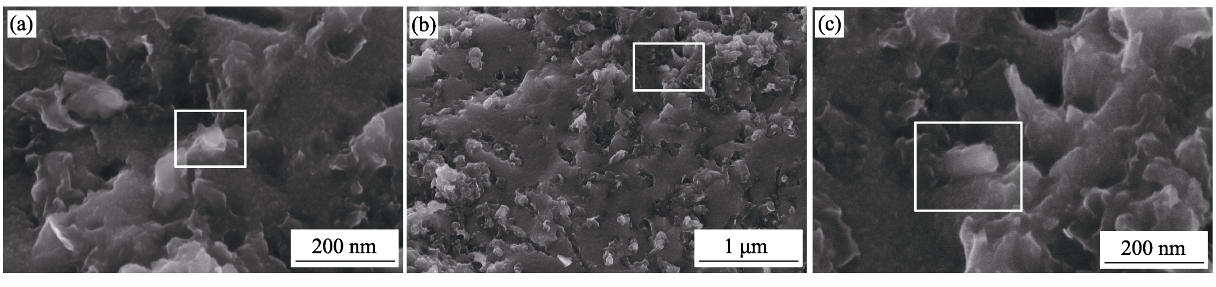

Fig. 3　SEM fractural morphologies of (a) as-grown SiC_{nw}, (b, c) BN-coated SiC_{nw} in composites
Local parts marked by white rectangular borders demonstrating that SiC_{nw} tends to break (a) or pull out (b, c)

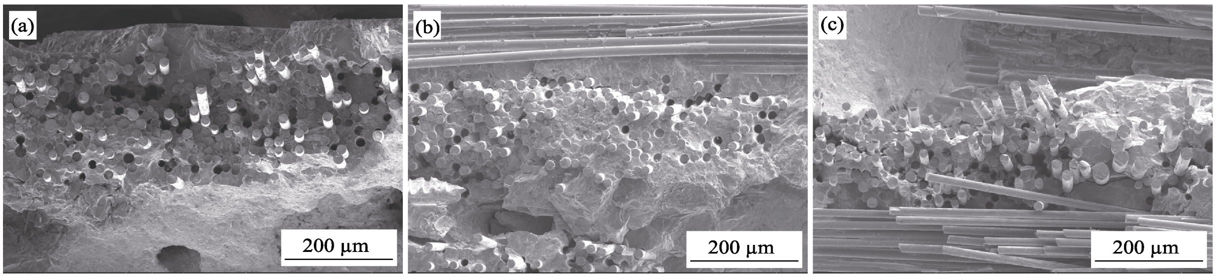

Fig. 4 Fracture morphologies of composite (a) SiC_f/SiC, (b) $SiC_f/SiC-SiC_{nw}$ and (c) $SiC_f/SiC-SiC_{nw}/BN$
The images demonstrating the pull-out length of fibers

behavior of materials owing to an increase of cracks propagation path and extra energy dissipation[13]. Li *et al.*[14] studied the modification effect of nanowires on composites and found their contribution to the absorption of breaking energy by rubbing against matrix after formation of obvious transverse cracks, which could transform otherwise mechanical catastrophic failure to ductile behavior. Such results may offer assistance to the discussion about AE diagrams in the following section.

2.3 AE diagrams and damage mechanisms

To get further understanding of the impact of SiC_{nw} on damage evolution of composites, AE measurement was performed in the three-point bending tests. The AE events with corresponding energy and numbers was detected and recorded, reflecting damage evolution such as generation and propagation of cracks. On basis of AE energy information, normalized cumulative AE energy *versus* stress curve are plotted to clarify damage threshold stress. Normalization is determined by the total energy of all AE events as denominator for every cumulative AE energy in specific stress. The slope of curve represents damage process rate[15]. As shown in Fig. 5, each type of composites shows different AE activities as external stress increases. For simplified analysis, the point highlighted by solid arrows where AE energy starts to be non-zero is denoted by σ_{min} (first AE stress), indicating the stress where the first AE signal is detected or the onset of microcrack generation. The other point highlighted by dotted arrows where the slope acquires a considerable increase is denoted by σ_{onset} (onset stress), representing the happening of severe damage inside composites like the formation of large transverse cracks and subsequent propagation[16-17]. All above mentioned values of three groups are listed in Table 2, it can be inferred from Fig. 5(b) that the introduction of SiC_{nw} delays the presence of σ_{min} as well as σ_{onset}. σ_{min} and σ_{onset} of $SiC_f/SiC-SiC_{nw}$ are 12.5% and 33.6% higher than that of original SiC_f/SiC, respectively. Besides, the deposition of BN interphase further enhances the hysteresis, for the values of $SiC_f/SiC-SiC_{nw}/BN$ shift to higher level compared with SiC_f/SiC by 34.5% and 47.4%, respectively.

The effect of SiC_{nw} can also be confirmed by stress-strain curves in Fig. 5. As is well-known, with external stress increasing, the traditional fracture mode of composites could be illustrated as following[18]: initial microcracks generate, microcracks propagate and merge into obvious transverse crack, fiber/matrix interfacial debonding, final fiber pull-out and breakage. The formation of transverse cracks makes main contribution to the transformation of stress-strain curve from linear part to non-linear part[15], namely, proportional limit as the knee point in this curve determines the stress where damage in composites starts to be severe and irreversible. By comparison, the proportional limit of $SiC_f/SiC-SiC_{nw}$ and $SiC_f/SiC-SiC_{nw}/BN$ are 20.9% and 61.4% higher

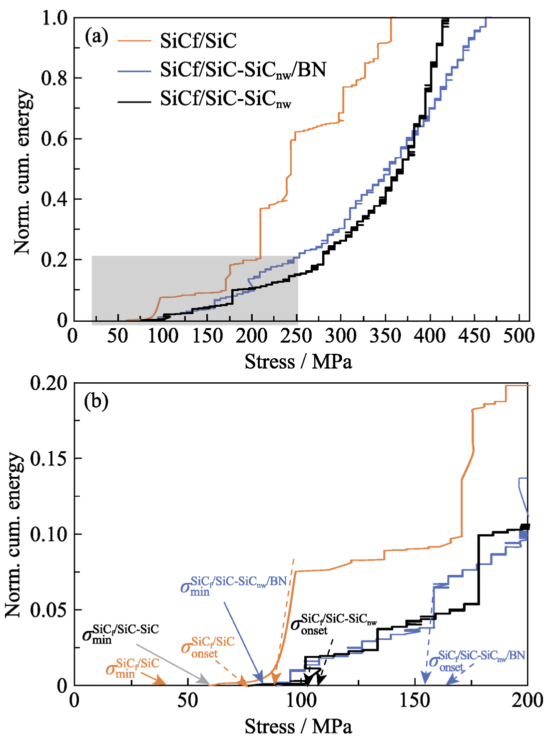

Fig. 5 Representative normalized cumulative AE energy curves as a function of stress (a) for composite SiC_f/SiC (orange), $SiC_f/SiC-SiC_{nw}$ (black) and $SiC_f/SiC-SiC_{nw}/BN$ (blue)
To clarify the difference of damage threshold among these three groups, initial key part (grey area) in (a) is magnified in (b). Colorful figures are available on website

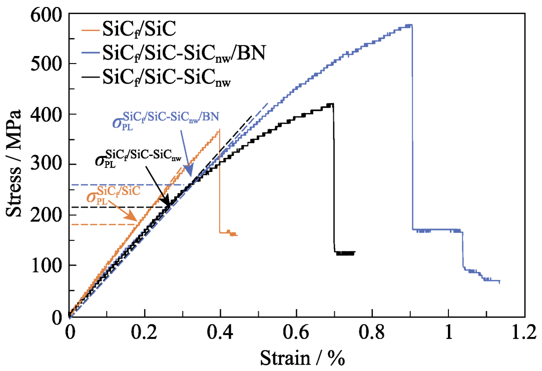

Fig. 6 Typical stress-strain curves of SiC_f/SiC(orange), $SiC_f/SiC-SiC_{nw}$ (black) and $SiC_f/SiC-SiC_{nw}/BN$ (blue)

The proportional limit is pointed out in the picture. Colorful figures are available on website

than that of original SiC_f/SiC, respectively, which roughly agrees with the differences of σ_{onset} values among these three types of composites. Therefore, AE results throw some light on detecting the important signal for identifying when composites bear noticeable interior damage. However, the stress recorded by AE is lower than proportional limit without exception, which may result from high sensitivity of AE devices, energy will be in record once high-energy event occurs, while one transverse crack is not enough for deviation from linear region in stress-strain curve.

Above analyses hint that early damage evolution is delayed, *i.e.*, the required stress for the formation of microcracks or transverse cracks is lifted by introducing SiC nanowires, and the restriction effect is more notable with the assistance of BN interphase. For confirming the assumption, the scattering diagram of individual AE events over time is demonstrated in Fig. 7. As is shown, the first detected AE activity is delayed in composites $SiC_f/SiC-SiC_{nw}$ and $SiC_f/SiC-SiC_{nw}/BN$ as anticipated, yet the obvious increase of AE activity representing the formation of apparent transverse crack does not show the same trend by comparison. With the aim of explaining the contradiction, Vickers Hardness test were performed to obtain information about crack propagation in composites. As shown in Fig. 8, after tests of same parameters, crack deflection and bridging are clearly observed in composites SiC_f/SiC, inferring that the cumulative fracture energy has been consumed and the seriously damaged matrix is brittle. By comparison, there are much less cracks caused by the indentation in composites $SiC_f/SiC-SiC_{nw}$ and $SiC_f/SiC-SiC_{nw}/BN$, the latter even obtain few cracks after the test, indicating that the fracture energy is far from enough for the formation of obvious cracks and subsequent propagation.

Considering observation given above, the inconsistence of previous assumption with AE scattering diagrams might be explained as following. In composites SiC_f/SiC and $SiC_f/SiC-SiC_{nw}/BN$, cracks tend to deflect along the weak-bonded BN interphase between fiber/matrix or nanowire/matrix, while in composites $SiC_f/SiC-SiC_{nw}$, cracks are more likely to be suppressed owing to the strong bonding between nanowires/matrix. In composite SiC_f/SiC, the propagation of cracks in brittle matrix is considerably fast, resulting in earlier presence of both the first recorded AE events and high-energy AE events, as confirmed in Fig. 7(a). On the other hand, as shown in Fig. 8(b, c), SiC_{nw} can effectively decrease the size of cracks by bridging between cracks, causing the improvement of σ_{min} and σ_{onset} in Fig. 5(b). In composites $SiC_f/SiC-SiC_{nw}$, nanowires tend to break as external stress increases, which brings forward the evident increase of AE activities. By contrast, due to the weak BN interphase in favor of sliding and pull-outs of nanowires, there are much more AE events recorded in composites $SiC_f/SiC-SiC_{nw}/BN$. The presence of rapid increase of AE activities is postponed, and the high-energy period lasts for a shorter time. It is also noteworthy that AE events gain an obvious boost after the hysteresis at early stage of damage evolution, which may result from the merging of microcracks or the breaking of short nanowires.

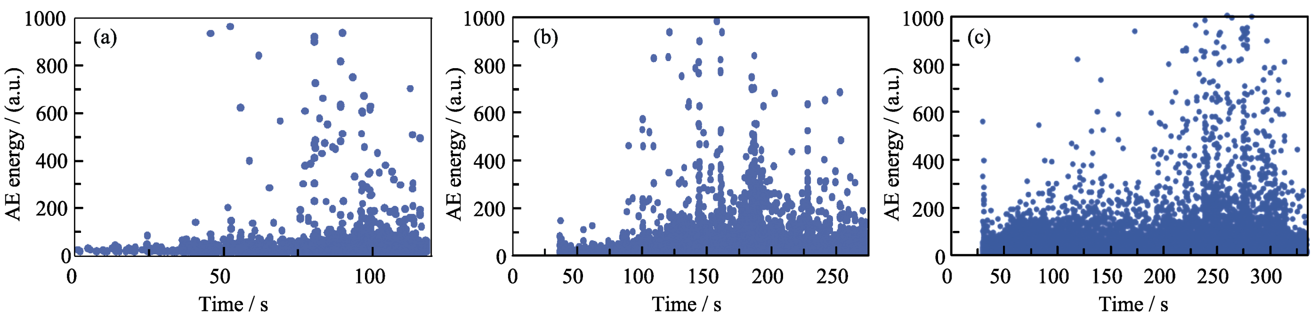

Fig. 7 Scatter diagrams of the energy of individual AE events as a function of time in composites (a) SiC_f/SiC, (b) $SiC_f/SiC-SiC_{nw}$, and (c) $SiC_f/SiC-SiC_{nw}/BN$

Considering the massive amount of data, diagrams are depicted after compression

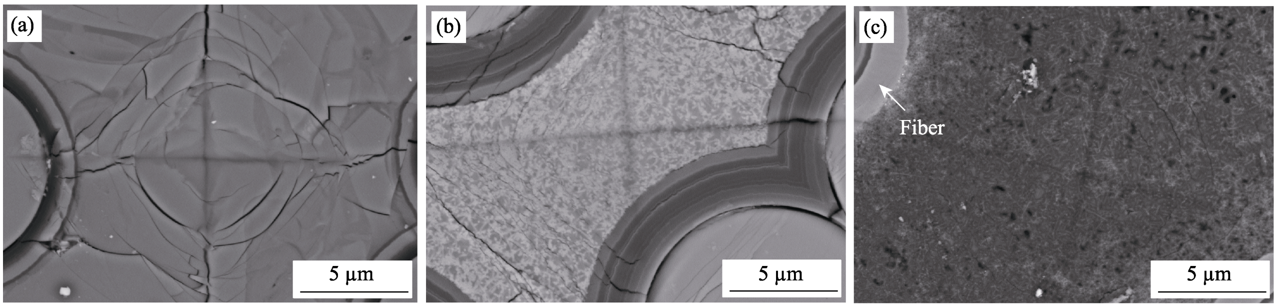

Fig. 8 SEM micrographs of crack propagation around the indentation in composites
(a) SiC_f/SiC; (b) $SiC_f/SiC-SiC_{nw}$; (c) $SiC_f/SiC-SiC_{nw}/BN$

3 Conclusions

SiC nanowires were introduced in composite SiC_f/SiC to realize a hierarchical structure. The modification effect of nanowires on microstructure and mechanical properties was investigated. Compared to original SiC_f/SiC, the density and porosity of $SiC_f/SiC-SiC_{nw}$ and $SiC_f/SiC-SiC_{nw}/BN$ are both positively optimized to a higher level. SiC nanowires wrapped by BN interphase significantly improve the fractural strength and proportional limit. AE results show that the proportional limit may correlates with onset stress of composites. With the assistance of Vickers Hardness Impresses, it is found that the reinforcing effect of SiC_{nw} may be attributed to delaying the presence of microcracks and bridging cracks. In addition, the resultant hindering effect of cracks of SiC_{nw} could not be fully optimized when SiC_{nw} are not coated with BN, although the brittle matrix is effectively enhanced. Thus, the strength of $SiC_f/SiC-SiC_{nw}$ is comparable to original composites SiC_f/SiC.

References:

[1] NASLAIN R. Design, preparation and properties of non-oxide CMCs for application in engines and nuclear reactors: an overview. *Composites Science and Technology*, 2004, **64(2):** 155–170.

[2] DICARLO J A, van ROODE M. Ceramic Composite Development for Gas Turbine Engine Hot Section Components. Proceedings of the ASME Turbo Expo 2006: Power for Land, Sea, and Air, F, 2006. Volume 2: Aircraft Engine; Ceramics; Coal, Biomass and Alternative Fuels; Controls, Diagnostics and Instrumentation; Environmental and Regulatory Affairs. Barcelona, Spain. May 8–11, 2006**:** 221–231.

[3] NASLAIN R R. Processing of non-oxide ceramic matrix composites: an overview. *Advances in Science and Technology*, 2006, **50:** 64–74.

[4] YIN X, CHENG L, ZHANG L, *et al*. Fibre-reinforced multifunctional SiC matrix composite materials. *International Materials Reviews*, 2017, **62(3):** 117–172.

[5] YANG W, ARAKI H, TANG C, *et al*. Single-crystal SiC nanowires with a thin carbon coating for stronger and tougher ceramic composites. *Advanced Materials*, 2005, **17(12):** 1519–1523.

[6] HU J, DONG S, FENG Q, *et al*. Tailoring carbon nanotube/matrix interface to optimize mechanical properties of multiscale composites. *Carbon*, 2014, **69:** 621–625.

[7] ZHU G, XUE Y, HU J, *et al*. Influence of boron nitride nanotubes on the damage evolution of SiC_f/SiC composites. *Journal of the European Ceramic Society*, 2018, **38(14):** 4614–4622.

[8] HE F, LIU Y, TIAN Z, *et al*. Carbon fiber/SiC composites modified SiC nanowires with improved strength and toughness. *Materials Science and Engineering: A*, 2018, **734:** 374–384.

[9] CHU Y, LI H, FU Q, *et al*. Oxidation protection and behavior of C/C composites with an *in situ* SiC nanowire-SiC-Si/SiC-Si coating. *Corrosion Science*, 2013, **70:** 285–289.

[10] ZHAO K, LI K, WANG Y. Rapid densification of C/SiC composite by incorporating SiC nanowires. *Composites Part B: Engineering*, 2013, **45(1):** 1583–1586.

[11] DONG R, YANG W, WU P, *et al*. Effect of reinforcement shape on the stress-strain behavior of aluminum reinforced with SiC nanowire. *Materials & Design*, 2015, **88:** 1015–1020.

[12] THOULESS M D, EVANS A G. Effects of pull-out on the mechanical properties of ceramic-matrix composites. *Acta Metallurgica*, 1988, **36(3):** 517–522.

[13] DE GREEF N, GORBATIKH L, GODARA A, *et al*. The effect of carbon nanotubes on the damage development in carbon fiber/epoxy composites. *Carbon*, 2011, **49(14):** 4650–4664.

[14] KANG S M, KIM W J, YOON S G, *et al*. Effects of the PyC interface coating on SiC nanowires of SiC_f/SiC composite. *Journal of Nuclear Materials*, 2011, **417(1/2/3):** 367–370.

[15] MORSCHER G N, SINGH M, KISER J D, *et al*. Modeling stress-dependent matrix cracking and stress-strain behavior in 2D woven SiC fiber reinforced CVI SiC composites. *Composites Science and Technology*, 2007, **67(6):** 1009–1017.

[16] WHITLOW T, JONES E, PRZYBYLA C. *In-situ* damage monitoring of a SiC/SiC ceramic matrix composite using acoustic emission and digital image correlation. *Composite Structures*, 2016, **158:** 245–251.

[17] MORSCHER G N. Stress-dependent matrix cracking in 2D woven SiC-fiber reinforced melt-infiltrated SiC matrix composites. *Composites Science and Technology*, 2004, **64(9):** 1311–1319.

[18] ARGON A S. Fracture of composites. *Treatise on Materials Science and Technology*, 1972, **1:** 79–114.

碳化硅纳米线增韧碳化硅纤维/碳化硅基体损伤行为研究

李陇彬[1,2], 薛玉冬[1,2], 胡建宝[1,2], 杨金山[1,2], 张翔宇[1,2], 董绍明[1,2]

(1. 中国科学院 上海硅酸盐研究所, 高性能陶瓷和超精密微结构国家重点实验室, 上海 200050; 2. 中国科学院大学 材料与光电研究中心, 北京 100049)

摘 要: 通过在碳化硅纤维表面原位生长纳米线得到具有多级增强结构的碳化硅复合材料, 对复合材料引入纳米线后的微观结构、弯曲强度以及损伤的变化过程进行了研究。研究结果表明, 相较于原始的碳化硅纤维增强碳化硅复合材料, 碳化硅纳米线可以明显提高基体沉积效率并改善材料的弯曲力学性能。从声发射技术和维氏硬度压痕测试结果可以看出, 纳米线通过抑制微裂纹的产生和在微裂纹之间发生桥联来抑制早期损伤的发展。此外, 在纳米线表面沉积一层氮化硼界面相, 纳米线与基体之间的结合力变弱, 复合材料对微裂纹的抑制和偏转得到进一步增强, 弯曲性能大幅提升。

关 键 词: 多级复合材料; 碳化硅纳米线; 力学性能; 声发射

中图分类号: TQ174　　**文献标志码**: A